

| | |
|--------------|---|
| Title | High-frequency characteristics and saturation electron velocity of InAlAs/InGaAs metamorphic high electron mobility transistors at high temperatures |
| Author(s) | Ono, Hideki; Taniguchi, Satoshi; Suzuki, Toshikazu |
| Citation | Proceedings of 16th International Conference on Indium Phosphide and Related Materials: 288-291 |
| Issue Date | 2004 |
| Type | Journal Article |
| Text version | publisher |
| URL | http://hdl.handle.net/10119/4157 |
| Rights | Copyright 2004 IEEE. Reprinted from Proceedings of 16th International Conference on Indium Phosphide and Related Materials, 2004. This material is posted here with permission of the IEEE. Such permission of the IEEE does not in any way imply IEEE endorsement of any of JAIST's products or services. Internal or personal use of this material is permitted. However, permission to reprint/republish this material for advertising or promotional purposes or for creating new collective works for resale or redistribution must be obtained from the IEEE by writing to pubs-permissions@ieee.org . By choosing to view this document, you agree to all provisions of the copyright laws protecting it. |
| Description | 2004 International Conference on Indium Phosphide and Related Materials : 16th IPRM : conference proceedings : May 31 (Mon.) - June 4 (Fri.), 2004, Kagoshima Shimin Bunka Hall, Kagoshima, Japan / sponsored by the Japan Society of Applied Physics, IEEE Lasers and Electro-Optics Society, and IEEE Electron Devices Society. |



HIGH-FREQUENCY CHARACTERISTICS AND SATURATION ELECTRON VELOCITY OF InAlAs/InGaAs METAMORPHIC HIGH ELECTRON MOBILITY TRANSISTORS AT HIGH TEMPERATURES

Hideki Ono, Satoshi Taniguchi, and Toshi-kazu Suzuki¹

*Advanced Devices R&D Department, Semiconductor Solutions Network Company, Sony Corporation
4-14-1 Asahi-cho, Atsugi-shi, Kanagawa, Japan +81-(0)46-230-5115, e-mail: Hideki.Ono@jp.sony.com*

¹ *Center for Nano Materials and Technology, Japan Advanced Institute of Science and Technology,
1-1 Asahidai, Tatsunokuchi, Ishikawa, Japan*

Abstract

We fabricated InAlAs/InGaAs metamorphic high electron mobility transistors (MHEMTs) with several indium contents. High-frequency performance of the MHEMTs was measured at high temperatures up to 473 K. By the delay time analysis, we have estimated saturation electron velocity. Temperature dependence of the saturation electron velocity for the MHEMTs with higher indium contents exhibits deviations from a theory.

I. Introduction

Metamorphic InGaAs devices grown on GaAs substrates, such as metamorphic high electron mobility transistors (MHEMTs), and metamorphic heterojunction bipolar transistors (MHBTs), are attractive candidates for micro- and milli-meter wave low noise and power applications as alternative to lattice-matched InGaAs devices grown on InP. The metamorphic device technology offers the performance advantage of InP devices and the cost advantage of GaAs devices. Recently, the MHEMT technology has been developed extensively to realize monolithic microwave integrated circuits (MMICs), such as low noise MMICs[1], and optoelectronic integrated circuits[2] on GaAs substrates. They exhibited good performance to compete with that of InP HEMT technology, despite of the crystalline defects existing in the device layers. Furthermore, the metamorphic device technology provides us a freedom of choice of indium content in the device design. For further development of the metamorphic device technology, the studies on basic characteristics of the metamorphic materials are important.

In the present work, using $\text{In}_x\text{Al}_{1-x}\text{As}/\text{In}_x\text{Ga}_{1-x}\text{As}$ MHEMTs, we have carried out a study on high-frequency characteristics and saturation electron velocity at high temperatures up to 473 K. The experiments were performed using MHEMTs with $x=0.36, 0.43, 0.53$, and lattice matched HEMTs (LMHEMTs, $x=0.53$) grown on an InP substrate to compare with the MHEMTs.

II. Material Characterization

The MHEMT structures, as shown in Fig. 1, were grown on semi-insulating (001) GaAs substrates by molecular beam epitaxy. Following the undoped graded InAlAs metamorphic buffer layer[3], the device structure incorporated a 200 nm undoped InAlAs layer, 15 nm undoped InGaAs channel, 6 nm undoped InAlAs spacer, Si delta-doping plane, 12 nm undoped InAlAs Schottky layer, and 50 nm n^+ -InGaAs cap layer. The active layer of the LMHEMTs has the same structure. The indium content of InGaAs channel, the root mean square (RMS) surface roughness, dislocation density, and Hall measurement results after recess etching are summarized in Table I. The indium contents were precisely determined by photoluminescence measurements taking into account quantized energy levels in the channels, and (004) and (115) X-ray diffraction measurements. In the metamorphic growth, surface with crosshatch is obtained. Figure 2 shows, as an example, the atomic force microscope (AFM) image of the MHEMT structure with indium content of 0.43. The RMS roughness of the MHEMTs is about $\sim 2-3$ nm. However, the roughness does not have negative effects on our device fabrications. From plan-view transmission electron microscope (TEM) observation, as shown in Fig. 3(a), we have found rather high-density crystalline defects in the active layers, threading dislocations and stacking faults. The density was typically on the order of 10^8 cm^{-2} , which is larger than that of the LMHEMTs by three orders of magnitude. Nevertheless, high electron mobility was obtained for the MHEMTs. This indicates that the defects

do not affect the electron velocity at low electric fields.

It should be noted that the defect density cannot be estimated from cross-sectional TEM observations, especially for the metamorphic materials with defect density $\lesssim 10^8 \text{ cm}^{-2}$ [4]. By the cross-sectional TEM observation, as shown in Fig. 3(b), it seems as if almost all dislocations were confined inside the buffer layer. We have carried out plan-view TEM observation of metamorphic materials supplied by many epi-vendors. As a result, we have found that, even in the best case, the defects on the order of 10^7 cm^{-2} is observed in the active layer of the metamorphic materials. Although there are some reports on MHEMTs or MHBTs with low defect density $\lesssim 10^6 \text{ cm}^{-2}$, we consider that these are underestimated results.

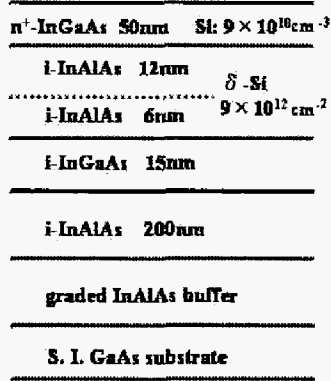


Fig. 1. The schematic cross section of the MHEMT structure.

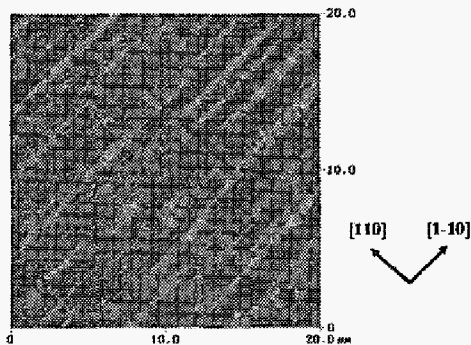


Fig. 2. Atomic force microscope image of the surface of the MHEMT with indium content of 0.43.

Table I. Indium content of InGaAs channel x , root mean square roughness R , threading dislocation density D , room temperature Hall mobility μ and sheet carrier density n_s of LMHEMTs and MHEMTs.

| x | 0.36 | 0.43 | 0.53 | 0.53/LM |
|--|-------------------|-------------------|-------------------|----------|
| R [nm] | 1.7 | 1.8 | 2.8 | < 1.0 |
| D [cm^{-2}] | 8.0×10^7 | 8.0×10^7 | 3.5×10^8 | $< 10^5$ |
| μ [cm^2/Vs] | 8100 | 8900 | 10300 | 10000 |
| n_s [10^{12} cm^{-2}] | 2.9 | 3.1 | 3.7 | 3.1 |

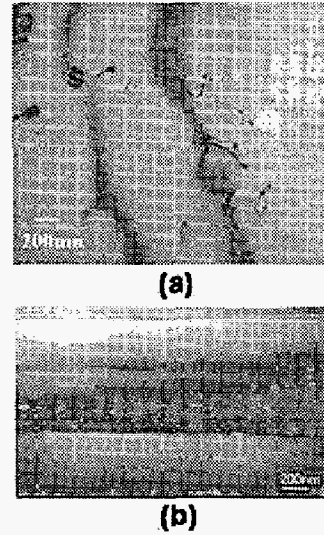


Fig. 3. Plan-view (a) and cross-sectional (b) TEM image for the MHEMT with indium content of 0.43.

III. Device Fabrication

The device fabrication was started with isolation by wet etching. The T-gate structures with gate length of 0.13–1.0 μm were realized by tri-layer resist process with electron-beam lithography. The gate length was precisely measured by critical dimension scanning electron microscopy. The selective wet recess etching was performed using mixture of adipic acid, ammonia and hydrogen peroxide[5]. After the recess etching, Pt/Ti/Pt/Au was deposited and lifted-off for the gate. Then alloyed Ni/AuGe/Au ohmic contacts were formed. Typically, the ohmic contact resistance was 0.35, 0.3, and 0.2 Ωmm for $x=0.36$, 0.43, and 0.53, respectively. Finally, Ti/Au contact pads were formed.

IV. Measurement and Analysis

High-frequency performance of the MHEMTs and the LMHEMT was measured at high temperatures ranging from 295 to 473 K. From the gate length L_g dependence of current gain cut-off frequency f_T at 295 K, $L_g \times f_T$ of 23, 27, and 32 GHz- μm is obtained for the MHEMTs with $x=0.36$, 0.43, and 0.53, respectively[6]. The temperature dependence of $L_g \times f_T$ is summarized in Fig. 4. The LMHEMTs exhibit the same behavior as that of the MHEMTs with $x=0.53$. When the devices were heated from 295 to 473 K, they showed $\sim 25\%$ decrease in $L_g \times f_T$.

In order to investigate saturation electron velocity, we performed the delay time analysis[7]. Figure 5 shows the relationship between the total delay time $\tau = 1/2\pi f_T$ and the reciprocal drain current density $1/I_D$ at 295 K, for the 1.0- μm -gate-length HEMTs with several indium contents. Saturation velocity transit time τ_{transit} is obtained by the linear extrapolation of the total delay time at infinite I_D . Figure 6 shows L_g dependence of τ_{transit} at 295 K, for the HEMTs with several indium contents. The saturation electron velocity v_s at high electric fields $\gtrsim 10$ kV/cm is evaluated by the relation $\tau_{\text{transit}} = (L_g + \Delta L)/v_s$, where ΔL is considered the spread of the depletion layer at the source and drain end of the gate. By applying the least-squares fitting to the data in the range of $0.2\mu\text{m} < L_g < 1.0\mu\text{m}$, v_s of 1.8×10^7 , 2.0×10^7 , and 2.5×10^7 cm/s is obtained for the MHEMTs with $x=0.36$, 0.43, and 0.53, respectively. Figure 7 shows L_g dependence of τ_{transit} at high temperatures up to 473 K, for the MHEMTs with $x=0.43$. As shown in Fig. 7, the slope of the line increases with an increase in temperature owing to v_s drop. Figure 8 shows temperature dependence of v_s . We obtained the same temperature dependence for the LMHEMTs and the MHEMTs with $x=0.53$. This indicates that defects in the MHEMTs do not affect the electron velocity at the high electric fields. The temperature dependence of v_s is theoretically given by

$$v_s \propto \left(\frac{eE_{\text{op}}/k_B T - 1}{eE_{\text{op}}/k_B T + 1} \right)^{1/2},$$

where E_{op} is optical phonon energy, and k_B is Boltzmann constant[8]. The solid curves in Fig. 8 are theoretical curves assuming E_{op} of 30 meV. However, at high temperatures, v_s of the MHEMTs with higher indium contents exhibits deviations from theoretical values. When the devices were heated from 295 K to 473 K, $L_g \times f_T$ and v_s show the decreases as summarized in Table II. For the MHEMTs with $x=0.43$ and 0.53, the decreasing rates of $L_g \times f_T$ and v_s are almost the same. Therefore, the reducing of the high-frequency performance at the high temperatures is mainly due to the drop in v_s . On the other hand, for the MHEMT with $x=0.36$, the decreasing rate of $L_g \times f_T$ is larger than that of v_s . This can be explained by the drop in mobility at the high temperatures.

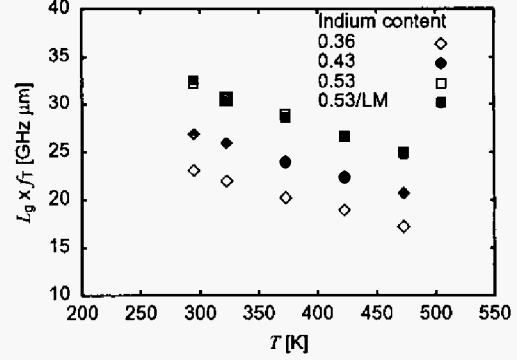


Fig. 4. $L_g \times f_T$ (L_g :gate length, f_T :cut-off frequency) as a function of temperature T for the HEMTs with several indium contents.

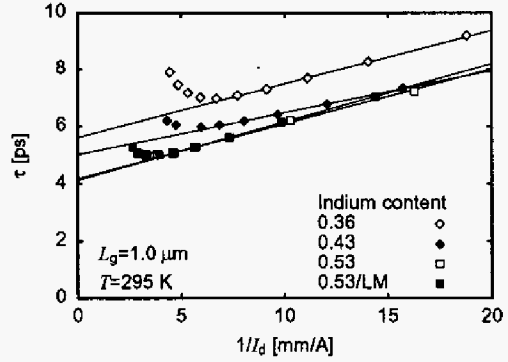


Fig. 5. Total delay time τ as a function of the reciprocal drain current density $1/I_D$ at 295 K for the 1.0- μm -gate-length HEMTs.

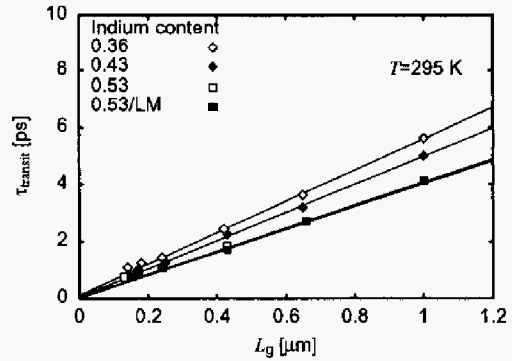


Fig. 6. Saturation velocity transit time τ_{transit} as a function of gate length L_g at 295 K.

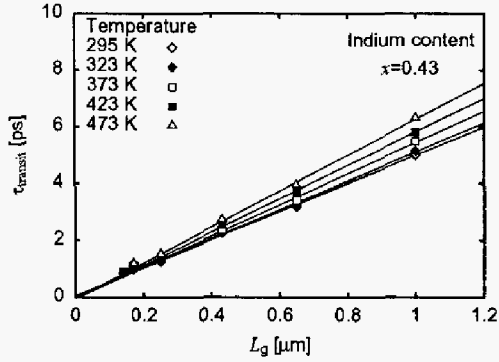


Fig. 7. Saturation velocity transit time τ_{transit} as a function of gate length L_g at high temperatures up to 473 K, for the MHEMTs with $x=0.43$.

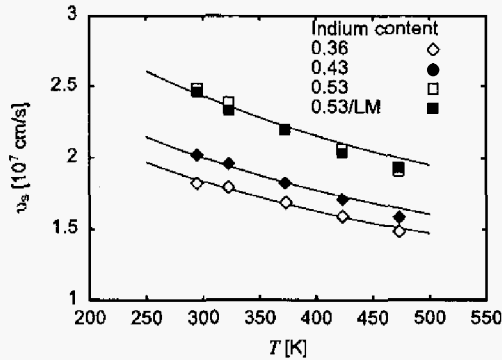


Fig. 8. Saturation velocity of electron v_s as a function of temperature T for InGaAs with several indium contents. The curves are calculated from the theory.

Table II. The decrease in $L_g \times f_t$ and v_s with an increase in temperature from 295 K to 473 K.

| x | 0.36 | 0.43 | 0.53 | 0.53/LM |
|------------------------------|------|------|------|---------|
| decrease in $L_g \times f_t$ | 26 % | 23 % | 23 % | 24 % |
| decrease in v_s | 19 % | 22 % | 23 % | 22 % |

V. Summary

High-frequency performance of InAlAs/InGaAs HEMTs with several indium contents was measured at high temperatures up to 473 K. By the delay time

analysis, we have estimated the saturation electron velocity. We have observed no difference between the LMHEMTs and the MHEMTs with $x=0.53$, despite of the defects in the active layer of the MHEMTs. The temperature dependence of measured saturation electron velocity for the MHEMTs with higher indium contents exhibits deviations from the theory. For the MHEMTs with $x=0.43$ and 0.53, the reducing of the high-frequency performance at high temperatures is explained by the drop in the saturation electron velocity.

Acknowledgment

The authors are grateful to S. Tomiya, T. Komoriya and J. Araseki for analysis of the metamorphic materials. They also thank T. Sasaki and H. Aihara for their help with fabricating the devices. This work was supported by International Collaboration Project at Center for Nano Materials and Technology (CNMT), Japan Advanced Institute of Science and Technology (JAIST).

References

- [1] C. S. Whelan, W. E. Hoke, R. A. McTaggart, S. M. Lardizabal, P. S. Lyman, P. F. Marsh, and T. E. Kazior: IEEE Electron Device Lett. **21** (2000) 5.
- [2] Y. Zhang, C. S. Whelan, R. Leoni, III, P. F. Marsh, W. E. Hoke, J. B. Hunt, C. M. Loughton, and T. E. Kazior: IEEE Electron Device Lett. **24** (2003) 529.
- [3] T. Mishima, K. Higuchi, M. Mori, and M. Kudo: J. Cryst. Growth. **150** (1995) 1230.
- [4] M. T. Bulsara, C. Leitz, and E. A. Fitzgerald: Appl. Phys. Lett. **72** (1998) 1608.
- [5] K. Higuchi, H. Uchiyama, T. Shiota, M. Kudo, and T. Mishima: Semicond. Sci. Technol. **12** (1997) 475.
- [6] H. Ono, S. Taniguchi, and T. Suzuki: Jpn. J. Appl. Phys. **43** (2004) *in press*.
- [7] T. Enoki, K. Arai, and Y. Ishii: IEEE Electron Device Lett. **11** (1990) 502.
- [8] P. A. Houston and A. G. R. Evans: Solid-State Electronics **20** (1977) 197.